

Optimal exercise frontier of Bermudan options by simulation methods

Dejun Xie*, David A. Edwards^{†,§} and Xiaoxia Wu[‡]

**Financial and Actuarial Mathematics
Xi'an Jiaotong Liverpool University, Suzhou, China*

*†Mathematical Sciences, University of Delaware
Newark, DE 19716, USA*

*‡Department of Mathematics
The University of Texas at Austin, Austin, USA*

Received: 13 September 2021; Accepted: 18 February 2022
Published: 14 April 2022

Abstract

In this paper, a novel algorithm for determining the free exercise boundary for high-dimensional Bermudan option problems is presented. First, a rough estimate of the boundary is constructed on a fine (daily) time grid. This rough estimate is used to generate a more accurate estimate on a coarse time grid (exercise opportunities). Antithetic branching is used to reduce the computational workload. The method is validated by comparing it with other methods of solving the standard Black–Scholes problem. Finally, the method is applied to two cases of Bermudan options with a second stochastic variable: a stochastic interest rate and a stochastic volatility.

Keywords: Simulation; Bermudan options; exercise boundary; antithetic branching; stochastic interest rate; Heston model.

1. Introduction

European options are financial contracts that grant the contract holder the right to exercise the contract (i.e., sell or purchase the underlying asset) at a specified strike price K *only* at the expiration date T of the contract. This lack of flexibility spurred the creation of American options, which allow *early exercise* at any time $t \leq T$.

[§]Corresponding author.

Email addresses: §dedwards@udel.edu

The added convenience and flexibility of an American option has a mathematical downside: the values of American options are difficult to determine.

Consequently, it may not be easy to decide the time t and asset price S_t at which the option should be exercised. In particular, there is an *early exercise boundary* $S_t = B(t)$ which determines the hold and exercise regions; this boundary casts the system as a moving boundary problem. The location of the early exercise boundary is important for practitioners because it contributes to the price of American-style financial derivatives, which are the most widely traded worldwide. Due to this derivative's significance and complexity, practitioners and researchers have continuously studied the moving boundary problem for American options.

The optimal exercise boundary for an American option has been much studied, particularly in the case of plain vanilla American options. The resulting ideas and numerical methods can be divided into three approaches. One approach is to formulize the problem with partial differential equations (PDEs), which are solved backwards in time from the point of maturity. Using this approach, Barles (1995), Kuske and Keller (1998), Stamicar *et al.* (1999), and Chen and Chadam (2007) provide analytical asymptotic equations for the optimal exercise boundary. The second approach is called the lattice method, and involves discretizing both t and S_t ; the binomial tree from Cox *et al.* (1979) and the trinomial tree from Boyle *et al.* (1989) are the most commonly discussed variations of this method. Although these two celebrated approaches have been widely applied to problems with low dimensions, they have not been used in problems with high dimensions because the computational time increases exponentially with dimension. To solve this "curse of dimensionality", a simulation approach was suggested in Boyle (1977), and subsequently was analyzed by Bossaerts (1989), Grant *et al.* (1997), Andersen (1999), and Ibanez and Zapatero (2004), among others. Our approach is a breakthrough in that it combines the simulation of a forward-looking property and dynamic programming with backward induction.

For the case of plain vanilla American put options, Fu (2001) provides numerical comparisons of different algorithms using the simulation approach, whereas Chen and Chadam (2007) stress different asymptotic results using PDEs, especially for near-expiry scenarios. It is generally agreed that the most successful method for this basic case appears to be the classical binomial tree method, as assessed by the criteria of stability, convergence, accuracy, and the insensitivity to extreme parameters (Sauer, 2012).

Bermudan options offer a compromise between the rigidity of the European option and the mathematical complexity of the American option. In a Bermudan option, early exercise is limited to a series of predetermined dates T_j . In this paper, we solve for the early exercise boundary of the Bermudan option using a simulation approach. We provide a convenient but realistically powerful tool to

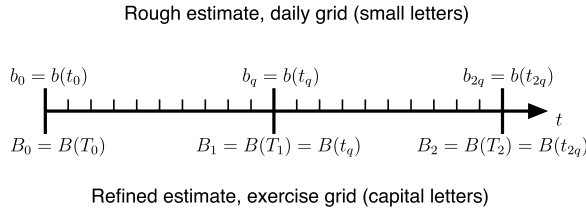


Fig. 1. Illustration of grids. The coarse estimate b will be calculated at each daily grid point t_j . The refined estimate B will be calculated only at the exercise dates T_j , which correspond to every q th daily point. (In this figure, $q = 10$.)

accurately estimate $B(t)$ by using a two-step process. First, we construct a fine daily mesh t_j on which we produce a rough estimate $B(t_j) = b_j$ for the exercise boundary. Then we calculate a more refined estimate $B(T_j) = B_j$ on a coarse (exercise) mesh consisting only of the early exercise dates (see Fig. 1).

Though the idea of using a Monte Carlo simulation is rather simple, its successful implementation in this paper requires a novel algorithm design, as we pay careful attention both to computing speed and convergence. For this purpose, an error reduction scheme utilizing antithetic branching is applied in our algorithm.

In order to validate our approach, we use the standard Black–Scholes Bermudan option to provide thorough numerical comparisons of our algorithm with both the binomial tree method and asymptotic solutions of the PDE approach. This allows us to establish the algorithm’s lower implementation cost and region of validity.

Accordingly, this paper is organized as follows. Section 2 introduces the problem in the framework of the free boundary setting. Section 3 presents the Monte Carlo simulation approach to find the optimal exercise boundary of Bermudan options. The algorithm is formulated from a stochastic control perspective and improved by an error reduction scheme, namely, antithetic branching. Then Sec. 4 applies our method to an example of the Bermudan put option under the Black–Scholes model, and provides comparisons of our simulation method to the existing asymptotic and binomial-tree results. In Sec. 5, we use our model to analyze the more complicated cases of Bermudan options with two stochastic variables: either a stochastic interest rate or a stochastic volatility under the Heston model (Heston, 1993). Our concluding remarks are given in Sec. 6.

2. Model Setup

We briefly outline the setup in the continuous-time context before introducing our numerical scheme. At time t , denote the underlying asset price by S_t . (We make the standard assumption that S_t is Markovian, i.e., the future asset prices depend on the current time but not on prior times.) When the underlying asset price S_t is equal to

Table 1. Notation dependent on grid.

Notation			
Continuous Time	Daily Grid	Exercise Grid	Description
t	t_j	$T_J = t_{qJ}$	time
	j	J	time index
$B(t)$	b_j	B_J	exercise boundary
	$m = qM$	M	time units at expiration
	n	N	number of realizations/paths
	i	I	index for realizations/paths
$P_t(s)$	$p_j(s)$	$P_J(s)$	payoff with asset price equal to s
$R(t)$	R_j		exercise region
S_t	S_j		asset price
$V_t(s)$		$V_J(s)$	option value underlying asset price equal to s
	$v(\hat{b}_j)$		option value with boundary starting at \hat{b}_j
	$\epsilon(\hat{b}_j)$	$\epsilon_J(\hat{s})$	error value used to compute boundary

s , we denote the value and payoff of the option at time t by $V_t(s)$ and $P_t(s)$, respectively.

At any possible exercise time t , the option holder must compare $V_t(s)$ and $P_t(s)$. If the option is worth more exercised than held, the buyer will exercise; this relationship defines an *exercise region* $R(t)$:

$$R(t) = \{s | P_t(s) > V_t(s)\} \tag{1}$$

which is bounded by an *exercise boundary* $s = B(t)$:

$$B(t) = \{s | P_t(s) = V_t(s)\}. \tag{2}$$

The focus of this paper is to estimate $B(t)$ numerically for Bermudan options; hence it is convenient to introduce two grids for time. First we construct a fine (daily) mesh t_j , assumed to be spaced one day apart, for $j = 0, 1, \dots, m$ (so t_m is the expiration date). Then we construct a coarse (exercise) mesh T_J of the exercise dates, for $J = 0, 1, \dots, M$ (so T_M is the expiration date). We assume that the exercise dates are spaced q days apart, so $T_J = t_{qJ}$. We retain throughout this convention that capital letters pertain to the exercise grid, while small letters pertain to the daily grid: see Table 1. (The remaining notation is listed in Table 2.)

3. Computing the Optimal Exercise Boundary

Though the exercise boundary $B(t)$ is defined for all time in the case of an American option, for the case of a Bermudan option, we need only the values $B_J = B(T_J)$ at the exercise dates. However, since the exercise dates are widely

Table 2. Other notation.

Notation	Description
c	volatility in stochastic models
E	realization set
$f(\tau)$	transformed exercise boundary in asymptotic results
k	ratio of interest rate to volatility effects
ℓ	time index for realization sets
p	time index
q	number of days between exercise dates
r	interest rate
s	given asset price
$\alpha(\tau)$	boundary function in asymptotics
κ	mean reversion rate in stochastic models
ξ	transformed time in asymptotics
ρ	correlation in stochastic models
σ	volatility
τ	scaled time to expiration
*	as a subscript on ϵ , used to represent a threshold
$\bar{\cdot}$	used to refer to a long-term mean
$\hat{\cdot}$	used to refer to provisional values
$\tilde{\cdot}$	used to refer to a discounted payoff
$\cdot^{(\cdot)}$	used to refer to paths, realizations, or experiments

spaced, to obtain an accurate approximation, we need information about the values $b_j = B(t_j)$ on the daily mesh.

In this paper, we take a two-pronged approach. Since they are not the dates of interest, on the daily mesh we construct only a rough estimate b_j —we don't waste computational effort generating a highly accurate estimate. There are fewer exercise dates, so we save our computational effort to generate highly accurate boundary estimates there. That's because these few dates are the only ones where actual financial decisions must be made. Hence, we have balanced the computational cost between the two grids.

To calculate the boundary values, we use a method of backward induction (dynamic programming recurrence). In other words, we work backwards from the expiration date, calculating the boundary along the way. As an introduction to the algorithm, we consider the last early exercise date before maturity: $J = M - 1$. (Since it is the final one, in this interval the Bermudan option behaves like a European one.)

3.1. Rough estimate: Final interval

We begin by computing the rough estimate for the boundary b_j . For now, we focus on the final interval between exercise dates: $t \in [T_{M-1}, T_M] = [t_{q(M-1)}, t_m]$.

Suppose that we are given an asset price $S_{M-1} = \hat{s}$ (how we obtain the value will be discussed in the next section). Given \hat{s} , we then generate n separate realization paths $S_p^{(i)}$ of the asset price on the daily mesh (here i indexes the paths).

To find the boundary b_j on the daily mesh for $t \in [t_{q(M-1)}, t_m]$, we work backwards from t_m . Therefore, at time t_j , we assume that all the b_p have been estimated for $p > j$. We next propose a value \hat{b}_j for b_j . This sequence of boundary values generates a proposed exercise region \hat{R}_j for $t \geq t_j$:

$$\hat{R}_j = R(\hat{b}_j, b_{j+1}, b_{j+2}, \dots, b_{m-1}, K), \tag{3}$$

where we have used the fact that $b_m = K$, since the exercise boundary always terminates at the strike price.

Then for each realization $S_p^{(i)}$, we need to know at what point t_p the option would be exercised. In particular, we find the *exercise set* E_p of all realizations for which the option would be exercised at t_p :

$$\begin{aligned} E_p(\hat{b}_j) &= \left\{ i \mid t_p \text{ is the first time } t_j \text{ that } S_j^{(i)} \in \hat{R}_j \right\} \\ &= \left\{ i \mid S_p^{(i)} \in R_p, i \notin E_\ell(\hat{b}_j) \text{ for } j \leq \ell < p \right\}. \end{aligned} \tag{4}$$

We note that E_p is specifically dependent on the choice of \hat{b}_j . This may seem strange since for any $p > j$, the boundary b_p has already been determined. But the realizations in E_p will be determined by those *not* in E_j , and this latter set definitely depends on \hat{b}_j .

This process is illustrated in Fig. 2 for a put option, where the exercise region is below the boundary. In this case, $i = 1$ would then belong to $E_{230}(\hat{b}_{226})$, $i = 2$ would belong to $E_{235}(\hat{b}_{226})$, and so on.

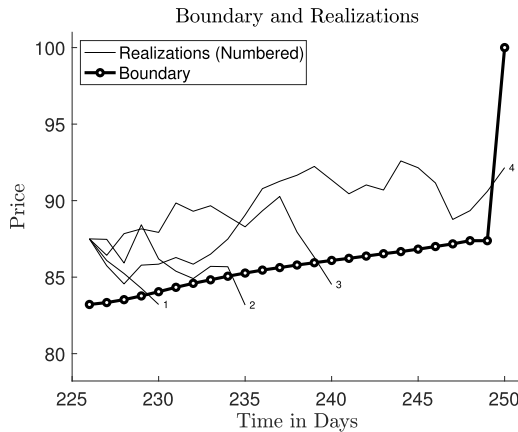


Fig. 2. One candidate for the rough boundary estimate b , along with four realizations of the asset walk. Here $j = 226$, $m = 250$. We use the parameters in Eq. (12a) along with $\hat{s} = 87.5$.

Given this expression, we may compute the value of the option at t_j , averaged over all the realizations. In particular, we add up the values of the option under each realization (indexed by i) and compute the average, which we denote $v(\hat{b}_j)$:

$$v(\hat{b}_j) = \frac{1}{n} \sum_{p=j}^m \sum_{i \in E_p(\hat{b}_j)} \tilde{P}(S_p^{(i)}). \quad (5)$$

Some remarks about Eq. (5) are appropriate.

- Technically, $v(\hat{b}_j) = V_{t=t_j}(\hat{s})$, given that the boundary is $\hat{b}_j, b_{j+1}, \dots, b_m$. We use our notation since the variable of interest here is \hat{b}_j .
- The inner sum represents the payoffs of all realizations exercised at t_p . If $p > j$, the payoff value must be discounted back to t_j . We use the tilde notation to indicate that discounting.

From Eq. (2), we know that at the actual exercise boundary, $V_t(s) = P(s)$. Therefore, it is natural to calculate the following error ϵ :

$$\epsilon(\hat{b}_j) = v(\hat{b}_j) - P(\hat{s}). \quad (6)$$

Then the estimated optimal exercise boundary b_j is chosen to be the value \hat{b}_j such that $\epsilon(\hat{b}_j)$ is arbitrarily close to 0, i.e.,

$$|\epsilon(\hat{b}_j)| < \epsilon_*, \quad (7)$$

where ϵ_* is an arbitrarily small number.

Therefore, the algorithm for the rough estimate is as follows:

1. Start with $J = M - 1$ and generate n realizations for the asset paths.
2. Start constructing the boundary with $j = m - 1$.
3. Construct an interval that contains the boundary values \hat{b}_j we wish to test. (In practice, this interval is taken as $[0, b_{j+1}]$ since the boundary is monotonic.)
4. Choose \hat{b}_j as the midpoint of the interval, and perform the procedure outlined above to determine $\epsilon(\hat{b}_j)$.
5. If Eq. (7) is not satisfied, use the sign of $\epsilon(\hat{b}_j)$ to bisect the interval of consideration, and repeat until convergence.
6. Decrement j until we have covered all j values down to $j = q(M - 1)$, which corresponds to $J = M - 1$, the first early exercise date.

3.2. Refined estimate: Final interval

When the algorithm outlined above has been completed, we will have the complete rough estimate for b_j (and hence R_j) on the daily mesh for the interval $[t_{q(M-1)}, t_{qM}]$ between the last two exercise dates. The left endpoint is also T_{M-1} ; we create a more accurate estimate B_{M-1} as follows.

Given some value \hat{s} of the asset price at the left endpoint $S_{q(M-1)}$, we again create a set of realizations for S on the daily mesh in this time period, this time N separate realization paths $S^{(l)}$. With all the R_j known, we calculate the average option value as before:

$$V_{M-1}(\hat{s}) = \frac{1}{N} \sum_{p=q(M-1)}^m \sum_{I \in E_p(b_{q(M-1)})} \tilde{P}(S_p^{(l)}). \quad (8)$$

Note the following differences from Eq. (5):

- Note that $j = q(M - 1)$, as we are solving on the exercise mesh.
- The hat is gone from the argument of the E sets, since b_j is now assumed known. Hence the arguments of the E sets are fixed, as we are now optimizing over \hat{s} .

Then analogous to Eq. (6), we define a new error

$$\epsilon_{M-1}(\hat{s}) = V_{M-1}(\hat{s}) - P(\hat{s}), \quad (9)$$

and choose the estimated optimal exercise boundary B_{M-1} to be the asset price \hat{s} such that $\epsilon_{M-1}(\hat{s})$ is arbitrarily close to 0, *i.e.*,

$$|\epsilon_{M-1}(B_{M-1})| < \epsilon_*. \quad (10)$$

3.3. The algorithm

Thus, the complete algorithm for the final interval is as follows:

- (i) Construct an interval that contains the asset values \hat{s} we wish to test. (In practice, this interval is taken as $[0, B_{J+1}]$ since the boundary is monotonic.)
- (ii) Choose \hat{s} as the midpoint of the interval, and run the algorithm in Sec. 3.1 to determine b_j for $j \in [q(M - 1), m]$.
- (iii) Then run the procedure outlined above to determine $\epsilon_{M-1}(\hat{s})$.
- (iv) If Eq. (10) is not satisfied, use the sign of $\epsilon_{M-1}(\hat{s})$ to bisect the interval of consideration for \hat{s} , and repeat until convergence.

After the computation for the final period, we now have a refined estimate B_{M-1} , which is an approximation to $B(T_{M-1})$. But now we can repeat the process outlined above for the larger interval $t_j \in [t_{q(M-2)}, t_m]$, which will yield a refined estimate of B_{M-2} . This process can be repeated working backwards until we reach time $t = 0$.

Note that there is no formal interpolation or projection of the results between grids. Rather, the rough estimates for the b_j are used directly in the algorithm in Sec. 3.2 to generate the refined estimate B_j .

We have to do n simulations on the daily mesh for each rough simulation; hence computational efficiency is essential. Therefore, for the rough simulations, we use

antithetic branching (Kroese *et al.*, 2013, Sec. 9.2). In this method, simulations are computed in pairs. The first is computed by a typical procedure with Wiener process(es) dW , while the second is computed by replacing dW with $-dW$. Hence, we need to generate only $n/2$ realizations to create n paths.

4. Numerical Results of Bermudan Put Option Under the Black–Scholes Model

Though we eventually want to use our method when the volatility or interest rate is stochastic, for validation purposes we begin by specializing to the case of standard Black–Scholes. In particular, we consider a Bermudan put option with standard payoff function

$$P(s) = \max(K - s, 0) \equiv (K - s)^+ \Rightarrow \tilde{P}(s) = e^{-r(t_m - t)}(K - s)^+, \quad (11a)$$

from which we have that the exercise region is given by

$$R(t) = \{s | s < B(t)\}. \quad (11b)$$

We choose the following Black–Scholes parameters:

$$K = 100, \quad r = 0.05, \quad \sigma = 0.3. \quad (12a)$$

We assume that the option has an expiration date 250 days in the future, and the option can be exercised every 25 days:

$$dt = \frac{1}{360}, \quad m = 250, \quad q = 25 \Rightarrow M = 10. \quad (12b)$$

Thus, the exercise boundary values that need to be estimated are $\{b_j\}_{j=0}^{250}$ and $\{B_j\}_{j=0}^{10}$. For our simulations, we take

$$n = 20000, \quad N = 50000, \quad \epsilon_* = 10^{-3}. \quad (12c)$$

With these parameters, we first choose an arbitrary $S_{225} = \hat{s}$ and \hat{b}_{249} ; then the very first step would be the calculation of Eq. (5):

$$v(\hat{b}_{249}) = \frac{1}{20000} \left[\sum_{i \in E_{249}(\hat{b}_{249})} (100 - S_{249}^{(i)}) + \sum_{i \in E_{250}(\hat{b}_{249})} e^{-r dt} (100 - S_{250}^{(i)})^+ \right]. \quad (13)$$

given \hat{s} . Note the following:

- At expiration, the boundary is the strike price, which is why K is the argument of the E .

- In this case, a realization falls in $E_{249}(\hat{b}_{249})$ if $S_{249}^{(i)} < \hat{b}_{249}$, and in $E_{250}(\hat{b}_{249})$ otherwise: hence there is no + superscript on the first term.

To compute b_{249} , we perform the algorithm as outlined in Sec. 3.1, stopping when Eq. (7) is satisfied for $\epsilon_* = 10^{-3}$, or when the interval of possible \hat{b} is narrower than 10^{-3} . Then by repeating the same process (working backwards) for $t_{248}, t_{247}, \dots, t_{225}$, we obtain the boundary in Fig. 2.

To compute B_9 , let $\{b_j\}_{j=225}^{250}$ be the previously calculated boundary shown in Fig. 2. For simplicity of exposition, suppose only the $N = 4$ paths shown are simulated. Then looking at each path individually, observe that paths 1–4 cross into the exercise region at $j = 230, 235, 241,$ and 250 , respectively. In this case, Eq. (8) becomes

$$V_9(\hat{s}) = \frac{1}{4} \left[\left(100 - S_{230}^{(1)}\right) e^{-(230-225)rt} + \left(100 - S_{235}^{(2)}\right) e^{-(235-225)rt} + \left(100 - S_{241}^{(3)}\right) e^{-(241-225)rt} + \left(100 - S_{250}^{(4)}\right) e^{-(250-225)rt} \right].$$

The boundary B_9 is the stock price \hat{s} such that

$$|V_9(\hat{s}) - (K - \hat{s})^+| < 0.001, \tag{14}$$

where we have used the value in Eq. (12c).

In reality, we use $N = 50000$ paths. Repeating the algorithm described above (working backwards) for T_j , we obtain the refined estimate $\{B_j\}_{j=0}^{10}$ on the exercise mesh. In order to reduce the possibility of spurious results, we perform the experiments 40 different times and declare the boundary to be the mean of the results.

The results for the standard Black–Scholes case are shown in Fig. 3. We note that the full curve $B(t)$ is constructed using simple linear interpolation; the rough

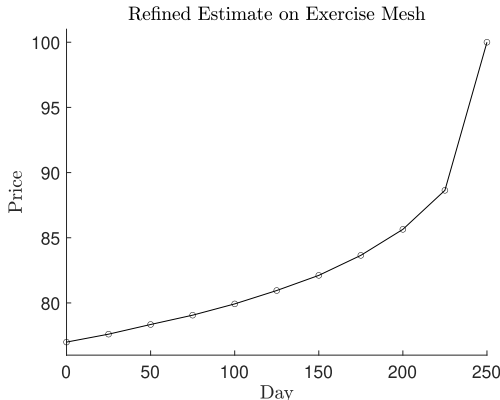


Fig. 3. Refined estimate for full range of t .

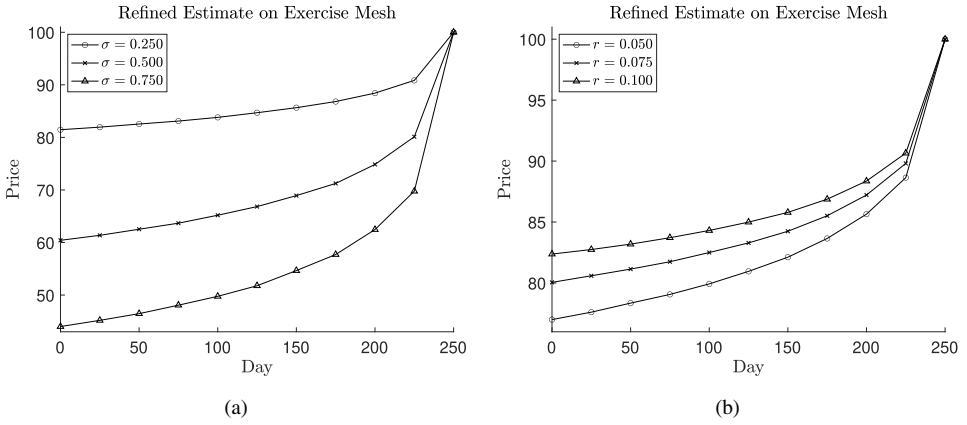


Fig. 4. Left (a): Exercise boundaries with parameters as in Eq. (12a), but with $\sigma = 0.25$, $\sigma = 0.5$, and $\sigma = 0.75$. Right (b): Exercise boundaries with parameters as in Eq. (12a), but with $r = 0.05$, $r = 0.075$, and $r = 0.1$.

estimates b_j are not used. The convexity of the curve is justified by many prior studies. Testing the curve for accuracy is performed in Sec. 4.1.

We illustrate the dependence of the boundary on the Black–Scholes parameters in Fig. 4. Figure 4(a) shows the effect of the underlying asset volatility σ . As expected, the exercise boundaries with smaller volatility stay above those boundaries that have larger volatility. That is, given high volatility, the asset prices dramatically fluctuate and early exercise is preferable only if the asset price is quite low.

In Fig. 4(b), as the value of the risk-free interest rate r increases, so does the exercise boundary. With a higher interest rate on risk-free assets, it is cost-effective to exercise the options for higher values of S , even though this means a smaller payout.

4.1. Comparisons with prior results

To establish the suitability of the antithetic branching technique, we compare the results from a simple Monte Carlo simulation with $n = 10000$ and $N = 50000$ realizations to those from the antithetic branching technique, where those same realizations can be leveraged into $n = 20000$ paths in a similar computational time. For each method, we performed 40 experiments, then computed the mean and standard error in the boundary position.

In Fig. 5, we present the difference between the mean and standard error of the two methods versus exercise date. The difference is quite small, and of course the antithetic branching approach gives more simulations in a smaller amount of time. Hence, for the rest of the paper, we use only antithetic branching for our approximations.

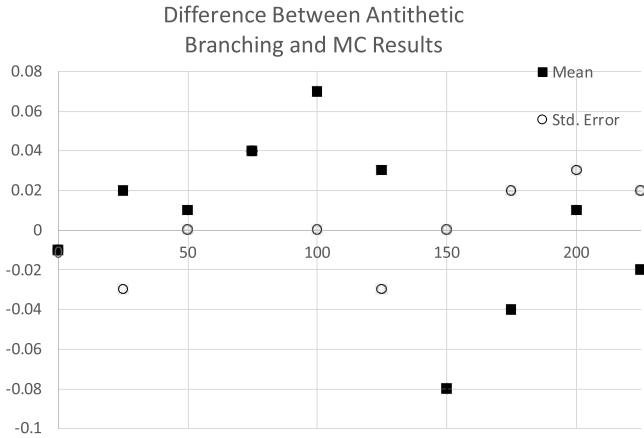


Fig. 5. Difference between the antithetic branching and simple Monte Carlo approach for the mean and standard error of B_j . Parameters are as in Eq. (12a).

Since the Bermudan put under Black–Scholes has been computed using other methods, we may use it as a benchmark to demonstrate the accuracy of our approximation. In particular, we compare our approach (results in Fig. 3) with the binomial tree from Cox *et al.* (1979) and approximations made by using the partial differential equations from Chen and Chadam (2007).

We embed the binomial tree method in Cox *et al.* (1979) into our algorithm. That is, when calculating the boundary, we simply replace the Monte Carlo approach with the binomial tree method. In particular, B_9 is found by continuously calculating $V_9(\hat{s})$ until Eq. (14) is satisfied. Once the binomial tree values of B_j have been calculated, they may be compared to our previous estimates (see Fig. 6).

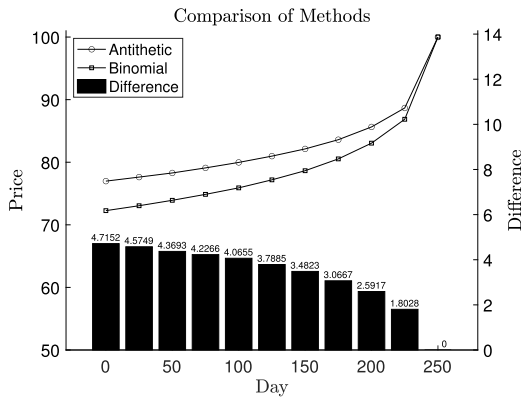


Fig. 6. Plots of exercise boundary using our method and the binomial tree method, using the left scale. Columns represent the error between the methods, using the right scale.

After comparing the boundaries obtained by the traditional binomial tree method and our simulation, we can draw the conclusion that our method is satisfactory, as the trends of the two boundaries are similar and the gaps between the two boundaries are small. In particular, the small change in the slope causes the two boundary estimates to converge as time runs backward from expiration (though the gap is never more than 5%). Thus, our estimate works better as time goes on.

Our method provides a conservative estimate for retaining the option: that is, the gap between the boundaries represents a larger exercise region for our method. The relatively larger boundary values obtained by our simulation can be blamed on the nature of the uncertainty caused in the Black–Scholes model. One can see that the general shape of the two boundaries is similar even though the boundary values derived from the binomial tree are relatively lower than the corresponding values derived from antithetic branching.

Though these results are promising, we further test our algorithm by comparing its approximations to the exercise boundary with asymptotic approximations obtained from the Black–Scholes equation. Let

$$\tau = \frac{\sigma^2(t_m - t)}{2}, \quad B(t) = Ke^{-f(\tau)}, \quad \alpha(\tau) = \frac{[f(\tau)]^2}{4\tau}.$$

Kuske and Keller (1998) derived the result that

$$9\pi k^2 \tau \alpha^2 e^{2\alpha} \sim 1, \quad \tau \rightarrow 0; \quad k = \frac{2r}{\sigma^2}, \quad (\text{KK})$$

which captures the dominant behavior of α , in particular that

$$\lim_{\tau \rightarrow 0} \frac{2\alpha(\tau)}{|\log \tau|} = 1.$$

Chen and Chadam (2007) proved that as $\tau \rightarrow 0$, $\alpha(\tau)$ has a more general asymptotic expansion based on Merton’s solution for the infinite horizon problem for the Bermudan put option:

$$\xi = -\alpha - \log \left(\frac{2}{\sqrt{\pi}} \int_0^{\sqrt{\alpha}} e^{-z^2} dz \right) + \log \left(\frac{e^\alpha + 2ke^{1/\alpha} \log(1 + k^{-1})}{e^\alpha + e^{1/\alpha}} \right), \quad (\text{CC})$$

where

$$\xi = \log \left(\sqrt{4\pi k^2 \tau} \right).$$

The error for this estimate is less than 2×10^{-3} at any time within 3 years of expiration.

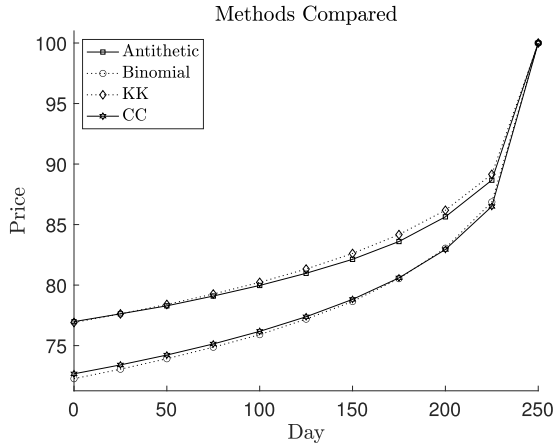


Fig. 7. Exercise boundaries for the Bermudan put using the parameters in Eq. (12a) for four different algorithms.

We compared the solution using our antithetic branching algorithm to the analytic solutions in (KK) and (CC); Fig. 7 contains a graph. The boundaries by the method of CC are viewed as “standard” solutions to the optimal exercise boundary for the Bermudan put option; note from Fig. 7 that the binomial-tree method is the most accurate. As observed, the boundary obtained by antithetic branching performs better than the KK method, even though it performed more poorly than the method of binomial trees.

Overall, these results give us confidence that our novel method can be used to accurately estimate the exercise boundary for Bermudan options, even in the case where there is more than one stochastic variable.

5. Nonstandard Examples of the Exercise Boundary of Bermudan Options

In the following subsections, we take advantage of our algorithm to obtain the exercise boundary for the Bermudan put option in two cases of higher dimensions. First we consider a stochastic interest rate following the CIR model (Cox *et al.*, 1985). Second, we consider a stochastic volatility following the Heston model (Heston, 1993). It is worthy to note that there is a tradeoff between the dimension of the boundary problem, the accuracy of the model and the computational time required to generate the boundary. For instance, the computational time for the Heston model is double the corresponding time for the Black-Scholes model, in part because the dimension of the Heston model is 2 and the Black-Scholes model’s dimension is 1.

5.1. Exercise boundaries of Bermudan put options with stochastic interest rates

Empirical evidence and studies show that the interest rate in the derivative market is dynamic and follows different stochastic models. Thus, obtaining the exercise boundary of the Bermudan put option under a stochastic interest rate is of practical interest. Typically, the interest rate follows the Vasicek model (Vasicek, 1977) or the CIR model (Cox *et al.*, 1985). The latter model is used in this paper, i.e.,

$$dS_t = r_t S_t dt + S_t \sigma \left[\sqrt{1 - \rho^2} dW_t^{(1)} + \rho dW_t^{(2)} \right], \quad S_0 = s, \quad (15a)$$

$$dr_t = \kappa(\bar{r} - r_t) dt + cr_t dW_t^{(2)}, \quad \sigma_0 > 0, \quad (15b)$$

where $\{W_t^{(i)}, t \leq T\}$, $i = 1, 2$ are two independent Wiener processes. Here $\rho \in [-1, 1]$ is the correlation between the stochastic asset price and the stochastic interest rate, \bar{r} is the long-term mean of the interest rate, and κ measures the rate at which a deterministic value would approach it. Lastly, c measures the size of the stochastic effects, and $\{\bar{r}, c, \kappa\}$ all satisfy the conditions that guarantee the existence of unique positive solutions for S_t and r_t .

We repeat the computational setup from the previous section, i.e., the Bermudan put option with 11 exercise opportunities and 40 different experiments. The stochastic interest rate is assumed not to correlate with the underlying asset, i.e., $\rho = 0$. Hence Eq. (15a) is replaced by

$$dS_t = r_t S_t dt + \sigma S_t dW_t^{(1)}. \quad (16)$$

We present three examples of the stochastic interest rate process: low-mean reversion and low volatility ($\kappa = 0.5$, $c = 0.03$), high-mean reversion and low volatility ($\kappa = 1$, $c = 0.03$), and high-mean reversion and high volatility ($\kappa = 1$, $c = 0.06$). In order to better compare with the constant-interest case, we took the initial rate r_0 to be equal to the long-term rate \bar{r} .

The results are shown in Fig. 8. Compared with the boundary for a constant interest rate, the boundary with a stochastic interest rate is nearly identical. Though not shown, the standard errors are also very close (with a deviation of less than 0.1 from the constant case). Hence we can conclude that the parameters of the CIR model have little effect on the optimal exercise boundary. This result agrees with Ibanez and Zapatero (2004), who concluded that assuming a stochastic interest rate process does not have a large impact on the price of put options because it is primarily influenced by the boundary position.

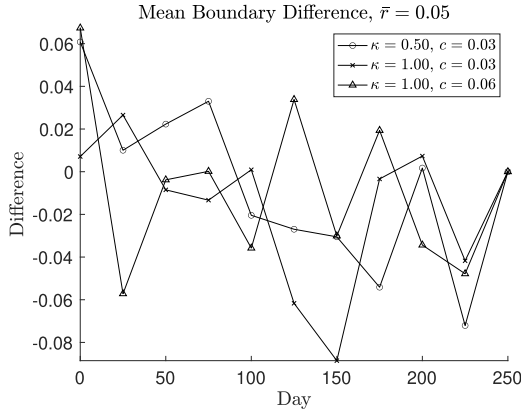


Fig. 8. Difference between mean of B_J in the stochastic interest rate context Eqs. (15b) and (16) and the case with constant r . Other parameters are as in Eq. (12a).

5.2. Exercise boundaries of Bermudan put options under the Heston model

Few works in the literature have discussed the exercise boundary for the Bermudan put option under stochastic volatility models, as the dimension of the problem has now increased. Such models are of great interest, as empirical research has proved that the volatility of the asset price in a financial market is not constant. However, such models are difficult to analyze. The method of partial differential equations is far more difficult to apply in this case. [Levendorskii \(2004\)](#) prices the Bermudan put option using Lévy processes, and [Beliaeva and Nawalkha \(2010\)](#) provide a “tree” approach to price Bermudan options under low-dimensional stochastic volatility models.

We use our algorithm to find the exercise boundary for the Bermudan put under the Heston model. In this case, the variance of the stock price is no longer constant but follows a CIR process, i.e.,

$$dS_t = rS_t dt + S_t \sigma_t \left[\sqrt{1 - \rho^2} dW_t^{(1)} + \rho dW_t^{(2)} \right], \quad S_0 = s, \quad (17a)$$

$$d\sigma_t^2 = \kappa(\bar{\sigma}^2 - \sigma_t^2) dt + c\sigma_t dW_t^{(2)}, \quad \sigma_0 > 0, \quad (17b)$$

where the variables are defined in analogous manner to those in Eq. (15). The only change is that in order for $\bar{\sigma}$ to be the long-term mean of σ , we change \bar{r} to $\bar{\sigma}^2$ in Eq. (17b).

Again we repeat the computational setup from the previous section, i.e., the Bermudan put option with 11 exercise opportunities and 40 different experiments. The stochastic volatility is assumed to correlate exactly with the underlying asset, i.e., $\rho = 1$. Hence, Eq. (17a) is replaced by

$$dS_t = rS_t dt + S_t \sigma_t dW_t^{(4)}. \quad (18)$$

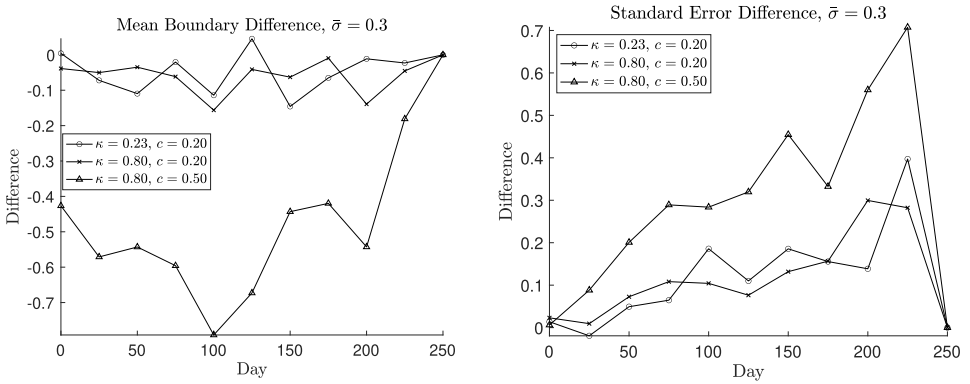


Fig. 9. Difference between mean (left) and standard error (right) of B_J in the stochastic volatility context and the case with constant σ . Here we use Eqs. (17b) and (18) with $\sigma_0 = 0.3$; the remaining stochastic model parameters are in the legend. Other parameters are as in Eq. (12a).

Three examples of the stochastic volatility process with an unchanged long-term rate of volatility are presented: low-mean reversion and low volatility of volatility ($\kappa = 0.23, c = 0.2$), high-mean reversion and low volatility of volatility ($\kappa = 0.8, c = 0.2$), and high-mean reversion and high volatility of volatility ($\kappa = 0.8, c = 0.5$). In order to better compare with the constant-volatility case, we took the initial rate σ_0 to be equal to the long-term rate $\bar{\sigma}$.

The results are shown in Fig. 9. At left we plot the difference between the mean boundary in the stochastic volatility and constant volatility cases using the same procedure as the one illustrated in Fig. 8. The differences are more pronounced than in the stochastic-interest case, and are generally negative. In other words, due to the increased variation in the volatility, the buyer should hold the option longer, in hopes of a further decrease in the asset price. Not surprisingly, the deviations are largest for the case of high c , where the stochastic effects are largest.

This same behavior with increasing c is shown at the right of Fig. 9, which shows a plot of the difference of the standard error in the same circumstances. Since σ_0 has the same value as in the constant-volatility case, the deviations start off small, growing larger over time before resetting to zero at expiration.

To determine the effect of the long-term mean $\bar{\sigma}$ on the boundary, we consider the case of low mean reversion and low volatility of volatility ($\kappa = 0.23, c = 0.2$). We generate the values of the boundary with both $\bar{\sigma} = 0.2$ and $\bar{\sigma} = 0.3$; the results are shown in Fig. 10.

We compute the mean boundary difference as in Fig. 9. Since c is small, we see that the deviations are small. We note that in the case $\bar{\sigma} = 0.2$, σ_0 is quite a bit larger than the long-term mean at first. Thus there is a larger deviation from the constant-volatility case where $\sigma = 0.3$. This mismatch means that the volatility is

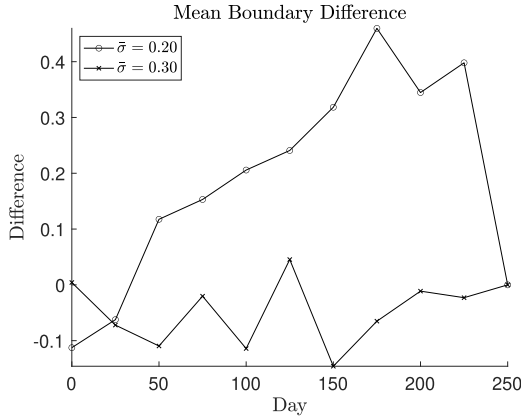


Fig. 10. Difference between mean of B_J in the stochastic volatility context and the case with constant σ . Here we use Eqs. (17b) and (18) with $\kappa = 0.23$, $c = 0.2$, $\sigma_0 = 0.3$. Other parameters are as in Eq. (12a).

larger than the long-term mean for a longer period of time. This period of increased volatility causes the boundary to shift (slightly) upward, indicating that the buyer should exercise earlier than in the constant-volatility case.

6. Conclusions and Further Research

In this paper, we described how to determine the optimal early exercise boundary for a Bermudan option, for which early exercise can happen only at select dates. We exploit this structure by constructing only a rough boundary estimate on the daily grid. On the coarse grid of early exercise dates where accurate data is actually needed, we use extra simulations to generate a more refined estimate. To reduce the variance and lengthy computational time, antithetic branching is used for the rough estimates.

To test our method, we consider a Bermudan put option under the Black–Scholes model. We compare the numerical results from our algorithm with results from the binomial tree method and certain analytical asymptotic results from the PDE approach. The comparisons show that our algorithm is both effective and accurate, though it slightly overestimates the boundary compared to the binomial tree method. It is important to note that we have limited the exercise opportunities in this paper, as our algorithm has this problem: the computational time scales exponentially as the number of exercise opportunities grows.

However, the advantage that our method has is that it can easily be adapted to more complicated situations where Black–Scholes does not apply, and the binomial method is too computationally expensive. In particular, we studied the case of

stochastic interest rates under the CIR model and stochastic volatility under the Heston model. By changing the parameters in the models, we can easily see their effect on the evolution of the early exercise boundary. The numerical results show that introducing a stochastic component to the interest rate has hardly any impact on the values of the exercise boundary. In contrast, introducing a stochastic component to the volatility induces larger changes to the boundary.

These results indicate that our method can be used to examine the early exercise boundaries for a wide range of problems. Further research will involve expanding the number of different models considered, as well as working to optimize our code's speed and efficiency.

Acknowledgments

The authors thank the reviewers for their helpful comments which greatly improved this paper.

References

- Andersen, L (1999). A simple approach to the pricing of Bermudan swaptions in the multifactor LIBOR market model, *Journal of Computational Finance*, 3(2), 5–32.
- Barles, G (1995). Critical stock price near expiration, *Mathematical Finance*, 5(2), 77–95.
- Beliaeva, NA and SK Nawalkha (2010). A simple approach to pricing American options under the Heston stochastic volatility model, *Journal of Derivatives*, 17(4), 25–43.
- Bossaerts, P (1989). Simulation estimators of optimal early exercise. Technical report, Carnegie Mellon University.
- Boyle, PP (1977). Options: A Monte Carlo approach, *Journal of Financial Economics*, 4(3): 323–338.
- Boyle, PP, J Evnine and S Gibbs (1989). Numerical evaluation of multivariate contingent claims, *Review of Financial Studies*, 2(2), 241–250.
- Chen, X and J. Chadam (2007). A mathematical analysis of the optimal exercise boundary for American put options. *SIAM Journal of Mathematics and Analytics*, 38(5), 1613–1641.
- Cox, JC, SA Ross and M Rubinstein (1979). Option pricing: A simplified approach, *Journal of Financial Economics*, 7(3), 229–263.
- Cox, JC, JE Ingersoll and SA Ross (1985). A theory of the term structure of interest rates, *Econometrica*, 53(2), 385–407.
- Fu, MC (2001). Pricing American options: A comparison of Monte Carlo simulation approaches, *Journal of Computational Finance*, 4(3), 39–88.
- Grant, D, G Vora and D Weeks (1997). Path-dependent options: Extending the Monte Carlo simulation approach, *Management Science*, 43(11), 1589–1602.
- Heston, SL (1993). A closed-form solution for options with stochastic volatility with applications to bond and currency options, *Review of Financial Studies*, 6(2), 327–343.

- Ibanez, A and F Zapatero (2004). Monte Carlo valuation of American options through computation of the optimal exercise frontier, *Journal of Financial and Quantitative Analysis*, 39(2), 253–275.
- Kroese, DP, T Taimre and ZI Botev (2013). *Handbook of Monte Carlo Methods*. Wiley Series in Probability and Statistics, Wiley.
- Kuske, RA and JB Keller (1998). Optimal exercise boundary for an American put option, *Applied Mathematical Finance*, 5(2), 107–116.
- Levendorskii, SZ (2004). Pricing of the American put under Levy processes, *International Journal of Theoretical and Applied Finance*, 7(3), 303–335.
- Sauer, T (2012). Numerical Solution of Stochastic Differential Equations in Finance. In JC Duan, WK Hardle and JE Gentle (eds.), *Handbook of Computational Finance*, Springer Handbooks of Computational Statistics, pp. 529–550. Springer.
- Stamihar, R, D Sevcovic and J Chadam (1999). The early exercise boundary for the American put near expiry: Numerical approximation, *Canadian Applied Mathematics Quarterly*, 7, 427–444.
- Vasicek, O (1977). An equilibrium characterization of the term structure, *Journal of Financial Economics*, 5(2), 177–188.